NUWC-NPT Technical Report 11,391
16 September 2002

Phase Sensitivity of Conventional Single-Mode, PANDA, and Holey Optical Fibers: A Comparison Study

Wilson K. S. Chiu
University of Connecticut

Jason M. Maguire
Marilyn J. Berliner
NUWC Division Newport

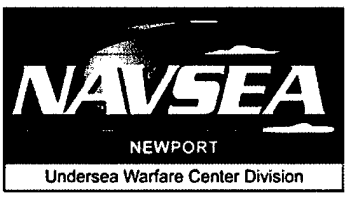

Naval Undersea Warfare Center Division
Newport, Rhode Island

PREFACE

This report was prepared under Project No. A132102, "Fishline Array," principal investigator Marilyn J. Berliner (Code 2141). The sponsoring activity is the Office of Naval Research (Code 321SS).

The technical reviewer for this report was Gregory H. Ames (Code 2141).

W. K. S. Chiu performed this work under the American Society of Engineering Education (ASEE) Summer Faculty Program sponsored by the Office of Naval Research.

Reviewed and Approved: 16 September 2002

Peter D. Herstein for

Ronald J. Martin
Head, Submarine Sonar Department

REPORT DOCUMENTATION PAGE

Form Approved
OMB No. 0704-0188

1. AGENCY USE ONLY *(Leave blank)*	2. REPORT DATE	3. REPORT TYPE AND DATES COVERED
	16 September 2002	

4. TITLE AND SUBTITLE
Phase Sensitivity of Conventional Single-Mode, PANDA, and Holey Optical Fibers: A Comparison Study

5. FUNDING NUMBERS
A132102

6. AUTHOR(S)
Wilson K. S. Chiu
Jason M. Maguire
Marilyn J. Berliner

7. PERFORMING ORGANIZATION NAME(S) AND ADDRESS(ES)
Naval Undersea Warfare Center Division
1176 Howell Street
Newport, RI 02841-1708

8. PERFORMING ORGANIZATION REPORT NUMBER
TR 11,391

9. SPONSORING/MONITORING AGENCY NAME(S) AND ADDRESS(ES)
Office of Naval Research
Ballston Centre Tower One
800 North Quincy Street
Arlington, VA 22217-5660

10. SPONSORING/MONITORING AGENCY REPORT NUMBER

11. SUPPLEMENTARY NOTES

12a. DISTRIBUTION/AVAILABILITY STATEMENT
Approved for public release; distribution is unlimited.

12b. DISTRIBUTION CODE

13. ABSTRACT (Maximum 200 words)

A comparison of phase sensitivity was conducted for three different types of optical-fiber designs having the same outer diameter. The optical fibers were subjected to a 1-μPa harmonic pressure load at excitation frequencies ranging from 1 Hz to 5 kHz. The polarization-maintaining and absorption-reducing optical fiber exhibited a marginal 6.3% gain in phase sensitivity over a conventional single-mode optical fiber. The holey fiber selected for this study showed a significant 130% phase sensitivity gain over conventional single-mode optical fiber, enabling the external harmonic load to strain the core beyond that observed in solid optical fibers.

14. SUBJECT TERMS
Fiber Optics
PANDA Fibers
Optical Fiber Signal Loss
Optical Fiber Strength
Holey Fibers
Single-Mode Optical Fibers
Optical Fiber Phase Sensitivity

15. NUMBER OF PAGES
17

16. PRICE CODE

17. SECURITY CLASSIFICATION OF REPORT	18. SECURITY CLASSIFICATION OF THIS PAGE	19. SECURITY CLASSIFICATION OF ABSTRACT	20. LIMITATION OF ABSTRACT
Unclassified	Unclassified	Unclassified	SAR

TABLE OF CONTENTS

LIST OF ILLUSTRATIONS

LIST OF TABLES

Table **Page**

LIST OF ABBREVIATIONS, ACRONYMS, AND SYMBOLS

ASMF	Air-silica microstructured fibers
E	Young's modulus
HF	Holey fiber
k_o	Free-space optical wave number
n_o	Refractive index
P	Ambient pressure
PANDA	Polarization-maintaining and absorption-reducing
PCF	Photonic crystal fibers
PM	Polarization maintaining
P_{11}, P_{12}	Pockel coefficients
SAP	Stress-applying part
SMF	Single-mode optical fiber
UV	Ultraviolet
WDM	Wavelength-division multiplexing

$\Delta\phi/P$	Change in phase
ε_{rr}	Radial strains
ε_{zz}	Axial strains
λ	Wavelength
ν	Poisson's ratio
ρ	Density
ϕ	Phase of light

PHASE SENSITIVITY OF CONVENTIONAL SINGLE-MODE, PANDA, AND HOLEY OPTICAL FIBERS: A COMPARISON STUDY

INTRODUCTION

The advent of specialty optical fibers with unique characteristics has inspired the study of the potential for and applicability of the use of such fibers as sensors. In recent years, two types of specialty optical fibers have shown a considerable increase in performance. Polarization-maintaining (PM) fibers allow signals to propagate in a fiber with minimal polarization dispersion. Holey fiber (HF) can be designed with minimal dispersion change across a wide range of wavelengths ($\lambda = 1.3 - 1.6$ μm) with reduced bending loss, and its internal hollow structure may significantly modify its sensitivity. A brief description of each fiber design is included in this report.

About 20 years ago, it was very difficult to use the phase or polarization state in the fiber for sensing because there was no way to control the polarization of a signal propagating in conventional single-mode optical fibers (SMFs). The advent of PM optical fibers dramatically increased the use of fiber optics in sensors, light communications systems, and integrated optical processing.[1-5] This report focuses on a particular PM fiber design: polarization-maintaining and absorption-reducing (PANDA) optical fibers. PANDA fibers are low-loss and low-crosstalk fibers that have the same core and cladding diameters as conventional SMFs. This design eliminates alignment and splicing loss associated with other (e.g., elliptical) PM optical fibers. The cross-section of a PANDA fiber illustrated in figure 1 shows a $2b$ cladding diameter fiber with a $2a$ diameter core. Two stress-applying parts (SAPs) composed of boron-doped fused silica at diameter t creates a large birefringence within the core. Sasaki et al.[6] have demonstrated a transmission loss of 0.22 dB/km and a crosstalk of –27 dB in a 5-km-long PANDA fiber at 1.56-μm wavelength. Their study evaluated the PANDA fiber's sensitivity to an acoustic wave, along with its PM capabilities. In particular, it evaluated how the presence of SAPs affect PANDA fiber performance as an underwater acoustic sensor.

Holey fiber, also known as air-silica microstructured fiber (ASMF) and photonic crystal fiber (PCF), was first fabricated in 1974 at Bell Laboratories by Kaiser and Astle.[7] It is composed of ultra-pure fused silica with air regions running along the length, but with a solid silica core. Three different HF structures are illustrated in figure 2.[8] The core guides a majority of the light. However, a significant amount of light travels down the air region by evanescent waves generated in the vicinity of the core. The predicted mode profiles in a holey fiber at 1.55 μm are shown in figure 3. Notice that the modes are not circular, but the size and arrangement of the holes can be tailored to change the mode field diameter by as much as three orders of magnitude,[9] reducing wavelength-dependent dispersion across $\lambda = 1.3 - 1.6$ μm, which is of interest to wavelength-division multiplexing (WDM) applications.[10] Windeler et al.[11] reported that holey fiber is extremely insensitive to bending loss. The authors observed no induced loss over 400 – 1600 nm when bent around a ¼-inch mandrel more than five times. Westbrook et al.[8] showed that Bragg gratings can

be ultraviolet (UV) written into photosensitive regions of various types of holey fibers. Abramov et al.[12,13] demonstrated a tunable fiber grating using holey fiber, with applications to WDM. Baggett et al.[14] recently compared large-mode holey and conventional fibers and found that between the two bending loss is comparable at 1.55 μm, while the holey fiber's weak wavelength dependence on dispersion offers a significant advantage for broadband applications where single-mode propagation is required. Additional features and possibilities of holey fibers are described by Monro et al.,[15] Bennett et al., [16] and Windeler and Ranka.[17]

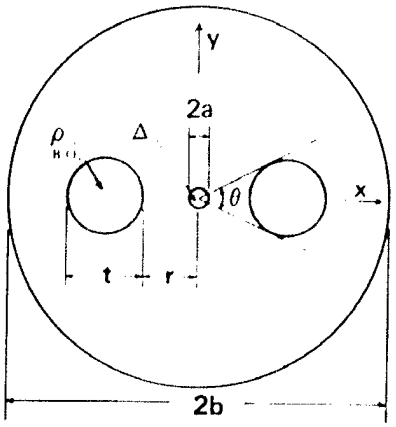

Figure 1. Structure of a PANDA Fiber[6]

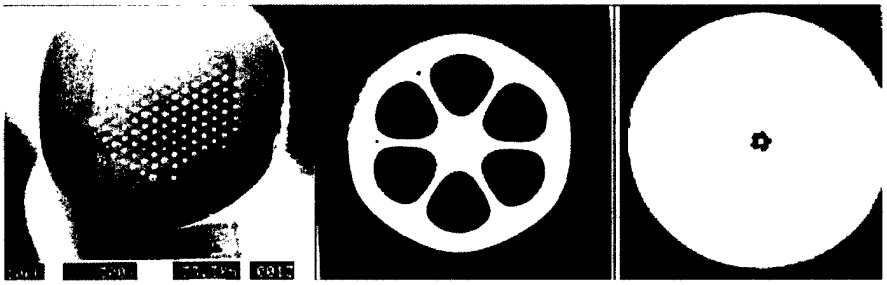

(a) small hole diameter (b) large hole diameter (c) small hole diameter and small number of holes

Figure 2. Micrographs of Three Different Types of Holey Fiber[8]

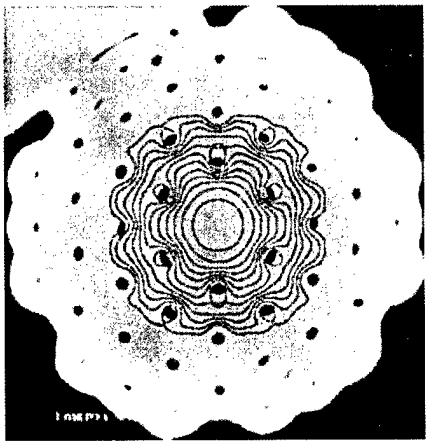

Figure 3. Predicted Light Mode Profiles at 1550 nm in a Holey Fiber[9]

Groups at Bell Laboratories (Lucent Technologies), the University of Southampton, the University of Bath, and several other institutions are actively researching this area. A literature review shows that this very young, but promising, field demonstrates potential for holey fiber use in undersea acoustic sensing. Specifically, holey fibers have reduced both dispersion sensitivity across a large range of wavelengths and bending loss. Further, UV gratings can be written into the HF core.

Since both PANDA and holey fibers offer attractive benefits over conventional single-mode fibers, the objective of this report is to study the response and sensitivity of these three different fiber designs to an acoustic wave. Following closely the work of Berliner,[18] the sensitivity of an optical fiber subjected to an external pressure field was derived. The phase of light ϕ passing through an undisturbed fiber of length L is defined as

$$\phi = n_o k_o L, \tag{1}$$

where n_o is the refractive index of the fiber's core, and k_o is the free-space optical wave number. When the optical fiber is exposed to an ambient pressure P, the external load induces a change in phase $\Delta\phi / P$ in the fiber, as expressed by

$$\frac{\Delta\phi}{P} = k_o n_o \Delta L + k_o \Delta n_o L. \tag{2}$$

In equation (2), the first term on the right represents a phase change induced by a change in the length of the fiber. The second term represents the photoelastic effect, where the change in the refractive index is induced by a mechanical strain.

Assuming that there are no shear stresses in the fiber, a *normalized change in phase* can be obtained by dividing equation (2) by equation (1) to obtain

$$\frac{\Delta\phi}{\phi P} = \varepsilon_{zz} - \frac{n_o^2}{2}\left[(P_{11} + P_{22})\varepsilon_{rr} + P_{12}\varepsilon_{zz}\right] . \quad (3)$$

The axial and radial strains on the fiber are ε_{zz} and ε_{rr}, respectively; P_{11} and P_{12} are the Pockel coefficients. Using $n_o = 1.45$, $P_{11} = 0.126$, and $P_{12} = 0.270$ in equation (3), one obtains

$$\frac{\Delta\phi}{\phi P} = \left|0.712\varepsilon_{zz} - 0.422\varepsilon_{rr}\right| . \quad (4)$$

Equation (4) is used to compare the response and sensitivity of three optical fibers—conventional single-mode, PANDA, and holey—to an acoustic wave. All three fibers evaluated had the same outer diameter and were coated with a similar thickness of urethane polyacrylate coating. These optical fibers were assumed to be infinitely long and were subjected to a harmonic pressure load. The pressure is axisymmetric and constant along the length of the fiber.

OPTICAL FIBER GEOMETRIES AND DIMENSIONS

All three optical fibers had an inner core and cladding section composed of pure or germanium-doped fused silica with the same outer diameter of 200 μm. In addition, a 20-μm-thick acrylate coating was added to each fiber, yielding a total outer diameter of 240 μm. Design variations for this study occurred within the 200-μm cladding/core region.

The SMF design had a solid cladding and core region, composed of a 5-μm- to 10-μm-diameter germanium-doped core surrounded by a pure fused-silica cladding. The PANDA design had two additional B_2O_3-doped fused-silica SAPs, as shown in figure 1. A specific PANDA fiber design was chosen from Sasaki et al.,[6] with the dimensions outlined in table 1.

Table 1. Dimensions of a PANDA Fiber

Dimensions from Figure 1	Value
$2a$	9.5 μm
$2b$	200 μm
R/a	4.1
t/b	0.61
Additional Acrylate Outer Coating (not shown in figure 1)	20-μm thick

The HF geometry shown in figure 2b was chosen for this study. Since HF designs are relatively new and immature, this design was chosen to ensure that the geometry was capable of being manufactured, and that Bragg gratings could be written into the design, as demonstrated by

Westbrook et al.[8] Dimensions for this design are shown in figure 4. The holey fiber was composed entirely of pure fused silica, with air pockets between the core and the cladding. The HF design was modified slightly from that used by Westbrook et al.[8] by expanding the outer diameter from 125 μm to 200 μm in order to properly compare the three fiber designs for phase sensitivity. However, the core diameter was kept the same to retain the holey fiber's light-guiding properties. The holey fiber was coated with a 20-μm-thick acrylate coating, yielding a total outer diameter of 240 μm. The acrylate coating is not shown in figure 4.

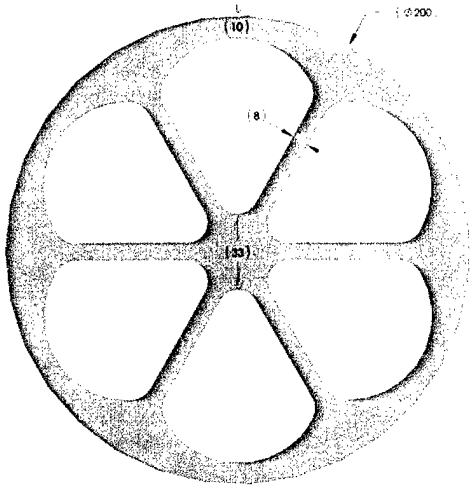

Figure 4. Dimensions of a Holey Fiber (in microns)

MATERIAL PROPERTIES

Conventional SMFs have a 5-μm- to 10-μm-diameter, approximately 5 vol% germanium-doped fused-silica cores, which can be approximated as pure fused silica. The SMF cladding is composed of pure fused silica. The PANDA fiber design has two additional SAPs (figure 1), which are composed of ~20% B_2O_3-doped fused silica. The holey fiber was composed of pure fused silica. As noted earlier, all three fiber designs were coated with a 20-μm-thick urethane polyacrylate outer layer, yielding an outer diameter of 240 μm.

The density (ρ), Young's modulus (E), and Poisson's ratio (ν) for each fiber are summarized in table 2. Pure fused silica and acrylate material properties were obtained from Berliner.[19] The SAP density was linearly extrapolated from data in Morey.[20] Since E and ν property data are not available for the SAP, it was assumed that the Poisson's ratio of 20% B_2O_3-fused silica was similar to that of pure fused silica. Since B_2O_3 has a lower Young's modulus than pure fused-silica glass, the Young's modulus of 20% B_2O_3-doped fused silica is taken to be 80% of that for pure fused silica. The Young's modulus approximation for the SAP produces a worst-case approximation, resulting in the phase sensitivity being over-predicted. It turns out that this

Table 2. Optical Fiber Materials and Properties

	Mechanical Properties		
Material	**ρ (kg/m^3)**	**E (N/m^2)**	ν
Core Pure fused-silica glass	2220	7.20×10^{10}	0.17
Cladding Pure fused-silica glass	2220	7.20×10^{10}	0.17
SAP 20% B_2O_3-doped fused silica	2135	5.76×10^{10}	0.17
Acrylate coating	1168	2.05×10^{9}	0.411

approximation does not significantly affect the solution since, as shown in the "Results and Discussion" section, the PANDA fiber design with this worst-case approximation did not show a significant increase in phase sensitivity as compared to the SMF design.

SOLUTION PROCEDURE

Due to the large length-to-diameter ratio of an optical fiber and the fact that the fibers evaluated in this study were not all axisymmetric, a two-dimensional model of the fiber cross-section was used since a three-dimensional model was not practical due to computational limits. All three fiber designs had two symmetric radial planes, which were orthogonal to each other. Hence, a solution was found for one quadrant, with symmetric conditions imposed at the orthogonal boundaries. A uniform pressure load was prescribed at the remaining circular boundary. This procedure allowed for a reduction in computational time and a refining of the mesh size in the existing computational domain to increase solution accuracy.

Since the pressure load was uniform along a finite length of fiber, a generalized plane strain assumption, which approximates a finitely long fiber that can displace in the axial and radial directions, was used. The axial strain in a generalized plane strain element is, however, uniform across the entire cross-section. Several element thickness values were examined, and an axial resonance mode was found that depended on the element length. To avoid the axial-induced resonant mode within the frequencies of interest, an element thickness of 100 meters was used.

Each of the three designs was created and meshed using Hypermesh, and analyzed using ABAQUS, a finite element analysis package. (See figure 5 for examples of meshed geometries for single-mode, PANDA, and holey fiber designs.) Element size was specified at ~1 μm, with

dominantly four-node bilinear quadrilateral elements. Fewer than five three-node linear triangle elements were used for each case. The problem size ranged from 6811 elements and 7145 nodes for the HF design to 11,875 elements and 12,090 nodes for the PANDA fiber design. The core region was intentionally meshed with only quadrilateral elements in order to increase accuracy in this area of interest.

RESULTS AND DISCUSSION

The three optical fibers were subjected to a 1-μPa harmonic pressure load to investigate the phase sensitivity of their designs in an underwater environment. All three fibers were 240 μm in diameter. Harmonic forcing was examined using a range of frequencies from 1 Hz to 5 kHz. The radial strain and axial strain (ε_{rr} and ε_{zz}) at the fiber core were calculated for each case and related to the normalized phase change $\Delta\phi/\phi P$ given by equation (4).

Stress fields for a 5-kHz load are shown in figure 5. The SMF showed a uniform stress field within the cladding, while the softer acrylate coating exhibited a lower, but uniform, stress distribution. The PANDA fiber exhibited characteristics similar to those of the SMF design, except that the SAP experienced a lower stress level due to its lower modulus. The holey fiber experienced a non-uniform stress load, with high-stress zones appearing both on the ribs connecting the core to the cladding and at the regions with the thinnest cladding. The HF stress distribution indicated that the harmonic pressure load can produce dramatically different stress distributions within the holey fiber, potentially affecting the strain within the fiber core.

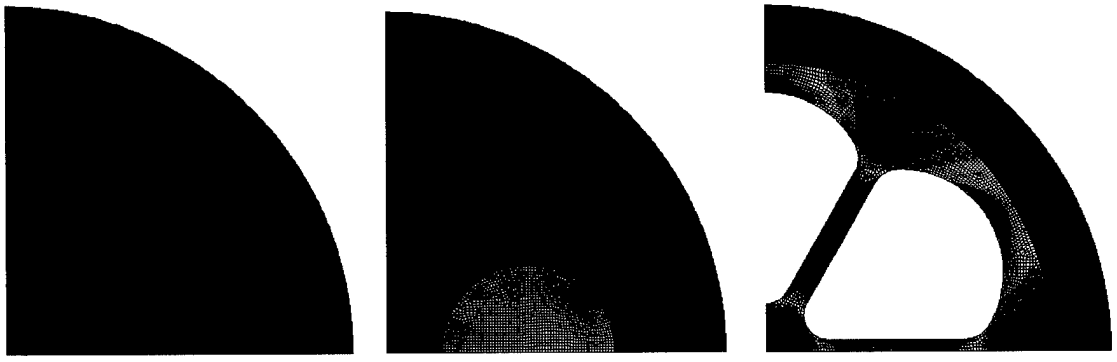

An external, 1-μPa, harmonic, uniform pressure load at 5 kHz was applied to the fiber. Red indicates high stress areas, while blue indicates low stress areas.

Figure 5. Mesh Structure and Stress Distribution for Single-Mode, PANDA, and Holey Fiber Designs

The axial strain (ε_{zz}) and the maximum radial strain (ε_{rr}) at the fiber center were predicted for the three fiber designs at 5 kHz (see figure 6). Small strain changes in the PANDA fiber were observed when compared to the SMF, but these changes resulted in an increase in phase sensitivity. Very significant differences in strain were observed for the holey fiber, with a 140% change in the axial direction and a 120% change in the radial direction relative to the SMF. The signed change occurred in such a way that the overall normalized phase sensitivity increased when using the holey fiber.

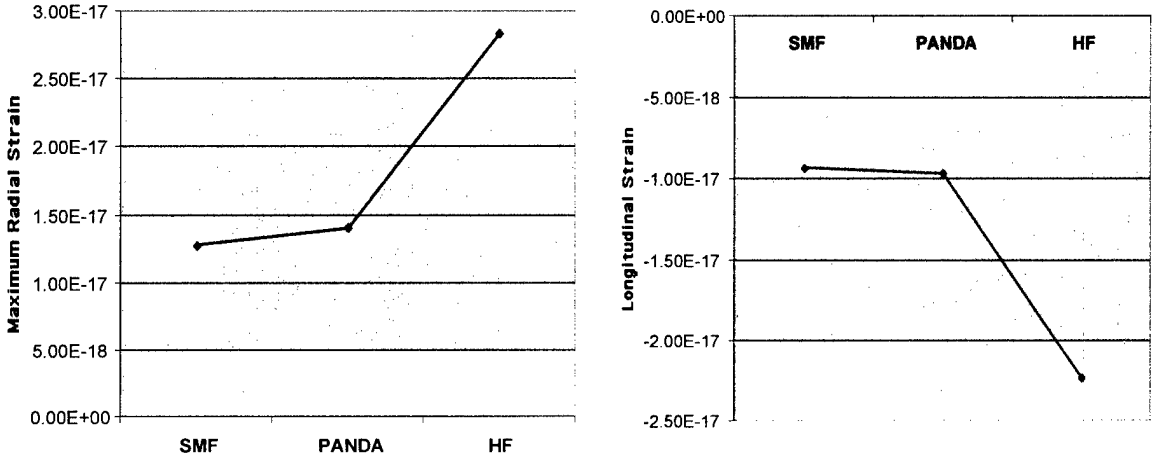

A 1-μPa, harmonic, uniform pressure load was used at 5 kHz.

Figure 6. Predicted Maximum Radial Strain ε_{rr} and Axial Strain ε_{zz} for Conventional Single-Mode, PANDA, and Holey Fibers

For all three designs, predicted radial shear strains were at least four orders of magnitude less than the axial and radial strains, thereby validating the normalized phase change formulation of equation (4). The radial strains predicted in the horizontal and vertical directions for the PANDA design differed by 16%, with the higher value occurring in the vertical direction. This is because the lower-modulus SAP imparts less stress in the horizontal direction, resulting in a lower radial strain in the horizontal direction. Since the goal is maximizing sensitivity, the maximum radial strain in the PANDA fiber was considered in this study. Interestingly, the HF design exhibited 0.4% difference in radial strain components. This may be due to the HF design's several symmetry planes in the azimuthal direction, which are not present in the PANDA design.

To determine the effect of excitation frequency on the normalized phase change, the predicted strains from figure 6 were inserted into equation (4) for excitation frequencies of 1 Hz to 5 kHz. No damping was imposed in this study. As depicted in figure 7, results for this frequency sweep showed that all three fiber designs had a constant phase sensitivity across the excitation frequencies of interest, which is highly desirable in acoustic sensor design. This is due to the absence of harmonic modes in this region, as was verified by calculating the natural frequency and corresponding harmonic modes of all three designs. This constant phase

sensitivity calculation predicted the first natural frequency mode occuring at >1 MHz, which is considerably above the range of interest of this study.

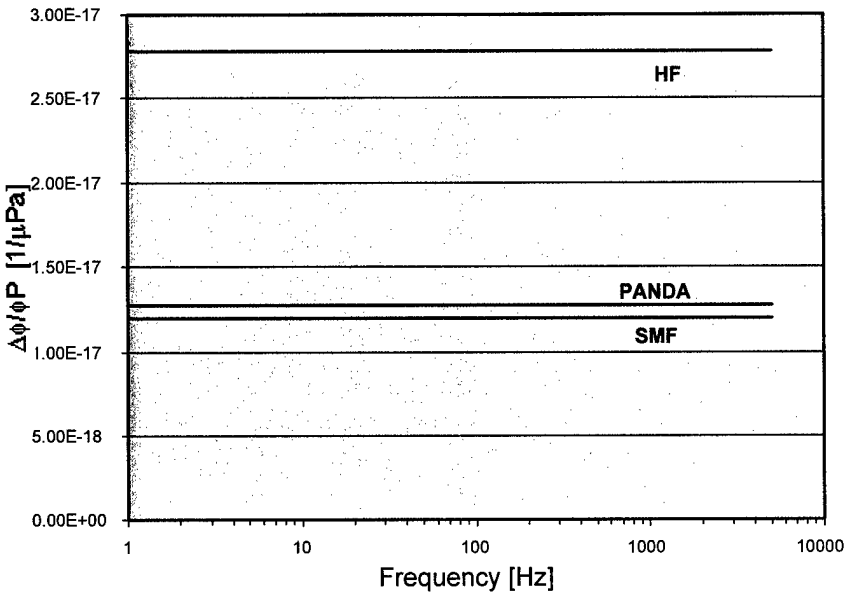

Figure 7. Phase Sensitivity for Single-Mode, PANDA, and Holey Fibers with a 1-μPa Harmonic Pressure Load

The predicted normalized phase change indicated that the PANDA design provides a 6.3% gain in phase sensitivity over the conventional SMF with the worst-case SAP property assumptions applied. The HF design offered a significant 130% gain in phase sensitivity over the SMF. This large gain is due to the increased axial and radial strains experienced by the HF design. Furthermore, this gain was flat across frequencies of 1 Hz to 5 kHz, making the HF design attractive for use in undersea acoustic sensors.

CONCLUSIONS AND RECOMMENDATIONS

A comparison of phase sensitivity was performed for three different optical fiber designs. The PANDA fiber exhibited a marginal 6.3% sensitivity gain over the conventional SMF. The holey fiber showed a significant sensitivity gain over the conventional SMF due to its fiber structure, with a predicted 130% improvement in phase sensitivity. Even though this study predicted that the HF design provides enhanced phase sensitivity, there are many other significant and unresolved issues that currently limit the use of holey fiber in acoustic sensors, such as attenuation, splicing, and connectorization.

This preliminary study was intended to demonstrate differences in phase sensitivity in selected optical fiber designs. Future work should include: (1) an investigation of the impact of cross-section optical fiber structures and dimensions on sensitivity; (2) a study focusing on optimizing a fiber geometry and dimensions; and (3) an examination of other important design aspects such as fabrication, handleability, attenuation, and their relationship to phase sensitivity.

REFERENCES

1. I. P. Kaminow, "Polarization in Optical Fibers," *IEEE Journal of Quantum Electronics,* vol. QE-17, no. 1, 1981, pp. 15-22.

2. S. C. Rashleigh, "Origins and Control of Polarization Effects in Single-Mode Fibers," *Journal of Lightwave Technology,* vol. LT-1, no. 2, 1983, pp. 312-331.

3. D. N. Payne, A. J. Barlow, and J. J. Ramskov Hansen, "Development of Low- and High-Birefringence Optical Fibers," *IEEE Journal of Quantum Electronics,* vol. QE-18, no. 4, 1982, pp. 477-488.

4. T. R. Wolinski, "Polarimetric Optical Fibers and Sensors," in *Progress in Optics XL,* E. Wolf, ed., Elsevier Science, New York, 2000.

5. J. Noda, K. Okamoto, and Y. Sasaki, "Polarization-Maintaining Fibers and Their Applications," *Journal of Lightwave Technology,* vol. LT-4, no. 8, 1986, pp. 1071-1089.

6. Y. Sasaki, T. Hosaka, M. Horiguchi, and J. Noda, "Design and Fabrication of Low-Loss and Low-Crosstalk Polarization-Maintaining Optical Fibers," *Journal of Lightwave Technology,* vol. LT-4, no. 8, 1986, pp. 1097-1102.

7. P. Kaiser and H. W. Astle, "Low-Loss Single-Material Fibers Made from Pure Fused Silica," *The Bell System Technical Journal,* vol. 53, 1974, pp. 1021-1039.

8. P. S. Westbrook, R. S. Windeler, C. Kerbage, and B. J. Eggleton, "Fabrication and Characterization of UV Written Gratings in Air-Silica Microstructured Fibers," *Bragg Gratings, Photosensitivity, and Poling in Glass Waveguides, OSA Technical Digest,* Washington, DC, 2001, pp. BWA1-1–BWA1-3.

9. N. G. R. Broderick, T. M. Monro, P. J. Bennett, and D. J. Richardson, "Nonlinearity in Holey Optical Fibers: Measurement and Future Opportunities," *Optics Letters,* vol. 24, no. 20, 1986, pp. 1395-1397.

10. T. M. Monro, D. J. Richardson, N. G. R. Broderick, and P. J. Bennett, "Holey Optical Fibers: An Efficient Model," *Journal of Lightwave Technology,* vol. 17, no. 6, 1999, pp. 1093-1102.

11. R. S. Windeler, J. L. Wagener, and D. J. DiGiovanni, "Silica-Air Microstructured Fibers: Properties and Applications," *Proceedings of the Optical Fiber Communication Conference,* vol. 4, 1999, pp. 106-107.

12. A. A. Abramov, B. J. Eggleton, J. A. Rogers, R. P. Espindola, A. Hale, R. S. Windeler, and T. A. Strasser, "Electrically Tunable Efficient Broad-Band Fiber Filter," *IEEE Photonics Technical Letters,* vol. 11, no. 4, 1999, pp. 445-447.

13. A. A. Abramov, A. Hale, R. S. Windeler, and T. A. Strasser, "Widely Tunable Long-Period Fibre Gratings," *Electronics Letters,* vol. 35, no. 1, 1999, pp. 81-82.

14. J. C. Baggett, T. M. Monro, K. Furusawa, and D. J. Richardson, "Comparative Study of Large-Mode Holey and Conventional Fibers," *Optics Letters,* vol. 26, no. 14, 2001, pp. 1045-1047.

15. T. M. Monro, P. J. Bennett, N. G. R. Broderick, and D. J. Richardson, "New Possibilities with Holey Fibers," *Proceedings of the Optical Fiber Communication Conference,* vol. 3, 2000, pp. 106-108.

16 P. J. Bennett, T. M. Monro, and D. J. Richardson, "Toward Practical Holey Fiber Technology: Fabrication, Splicing, Modeling and Characterization," *Optics Letters,* vol. 24, no. 17, 1999, pp. 1203-1205.

17. R. S. Windeler and J. K. Ranka, "Novel Properties of Air-Silica Microstructure Optical Fibers," *Proceedings of the Optical Fiber Communication Conference,* vol. 3, 2000, pp. 104-105.

18. M. J. Berliner, "Comparison of the Simulated Phase Sensitivity of Coated and Uncoated Optical Fibers from Plane-Strain Vibration and Static Pressure Models," NUWC-NPT Technical Report 11,147, Naval Undersea Warfare Center Division, Newport, RI, 7 June 1996.

19. M. J. Berliner, "An Analysis of Optical Phase in Coated Optical Fibers Using a Physics-Based Model of Wave Propagation in Composite Cylinders," NUWC-NPT Technical Report 11,224, Naval Undersea Warfare Center Division, Newport, RI, 5 May 2000.

20. G. W. Morey, *The Properties of Glass*, 2nd Edition, Reinhold Publishing Co., New York, 1954.

DISTRIBUTION LIST

	No. of Copies
Defense Technical Information Center	12
Naval Research Laboratory (A. Dandridge)	1
Office of Naval Research (ONR) (R. Elswick (Code 321))	1
University of Connecticut, Storrs (W. Chiu)	5